U.S. DEPARTMENT OF THE INTERIOR
U.S. GEOLOGICAL SURVEY

Basement Structure Beneath Langford Well Lake Basin, Fort Irwin, California, Based on Inversion of Gravity data.

By Robert L. Morin[1]

Open–File Report 00–518

2000

U.S. DEPARTMENT OF THE INTERIOR
BRUCE BABBITT, Secretary

U.S. GEOLOGICAL SURVEY
Charles G. Groat, Director

[1] U.S. Geological Survey, 345 Middlefield Road, Menlo Park, CA 94025

TABLE OF CONTENTS

ILLUSTRATIONS

TABLES

INTRODUCTION

Gravity data were used to study the basement structure of Langford Well Lake basin at the U.S. Army National Training Center, Fort Irwin, California. Figure 1 shows the location of the study area. During 1996 and 1999, 290 new gravity stations were measured. These data were merged with existing data to produce a depth–to–basement map, which, in turn was converted to a structure map of the basement surface below alluvial fill. This information can be used to help interpret water flow and reservoir capacity of the basin. In addition, gravity gradients were used to suggest locations of faults through or below alluvial fill. These gradients may be evidence for repositioning or extending mapped faults.

The locations of gravity stations are shown in figure 2 plotted on a colored grid of topographic elevations generated from 30 m DEM's (Digital Elevation Models). As shown by figure 3, gravity data used in this study are sufficiently accurate to permit 1–mGal contour intervals. Much of the older regional data in this study area are of lesser quality although they were included because they sufficiently represent regional gravity.

ACKNOWLEDGMENTS

Greg Smith provided much assistance in collecting and processing the gravity data.

GRAVITY REDUCTION

Conversion from meter readings to milligals was made using factory calibration constants. The meter used in the 1996 survey has an additional calibration factor determined by multiple gravity readings over the Mt. Hamilton calibration loop east of San Jose, Calif. (Barnes and others, 1969). Observed gravity values were based on an assumed linear drift between successive base readings. Vertical and horizontal controls were made by two techniques. The data collected in 1996 were established with laser surveying equipment, which has a vertical accuracy of about 0.1 m. The horizontal and vertical controls of the data collected in 1999 were made with a precision GPS system which also has a vertical accuracy of about 0.1 m.

Theoretical gravity at sea level is based on the Geodetic Reference System 1967 (GRS 67) (International Association of Geodesy, 1971, p. 58) for the shape of the spheroid. The datum for the observed gravity is the International Gravity Standardization Net 1971 (IGSN 71) (Morelli, 1974. p. 18). Observed gravity was calculated by adding meter drift and earth–tide corrections to the milligal equivalent meter readings. Free–air anomalies were calculated by subtracting the theoretical gravity from the observed gravity and adding the free–air correction as defined by Swick (1942, p. 65). Simple Bouguer anomalies were calculated by subtracting the Bouguer correction from the free–air anomaly. The Bouguer correction accounts for the attraction of rocks between the station and sea level, using a rock density of 2.67 g/cm^3.

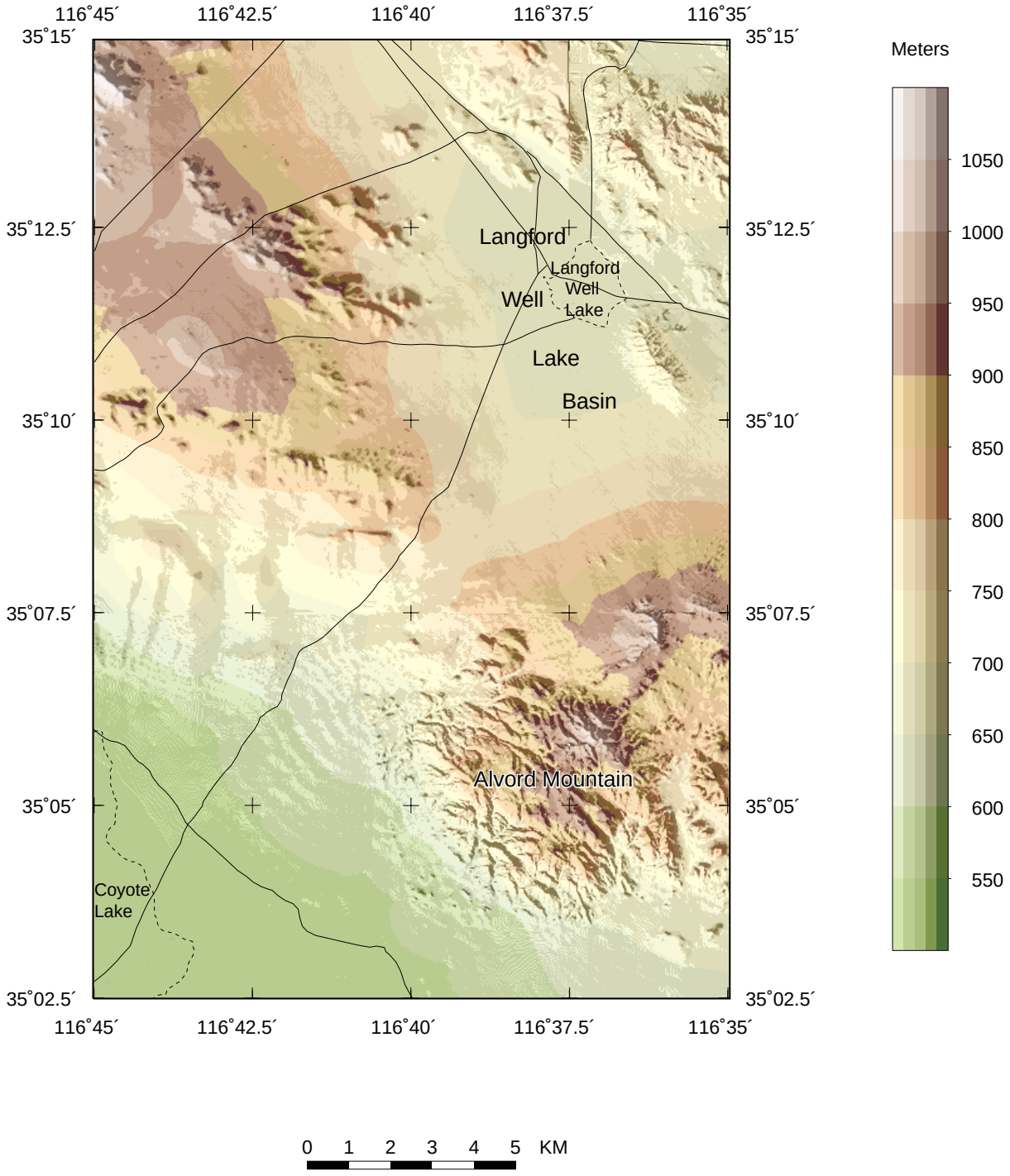

Figure 1. Topographic map of study area. Solid lines, selected roads; dashed lines, edges of lake beds.

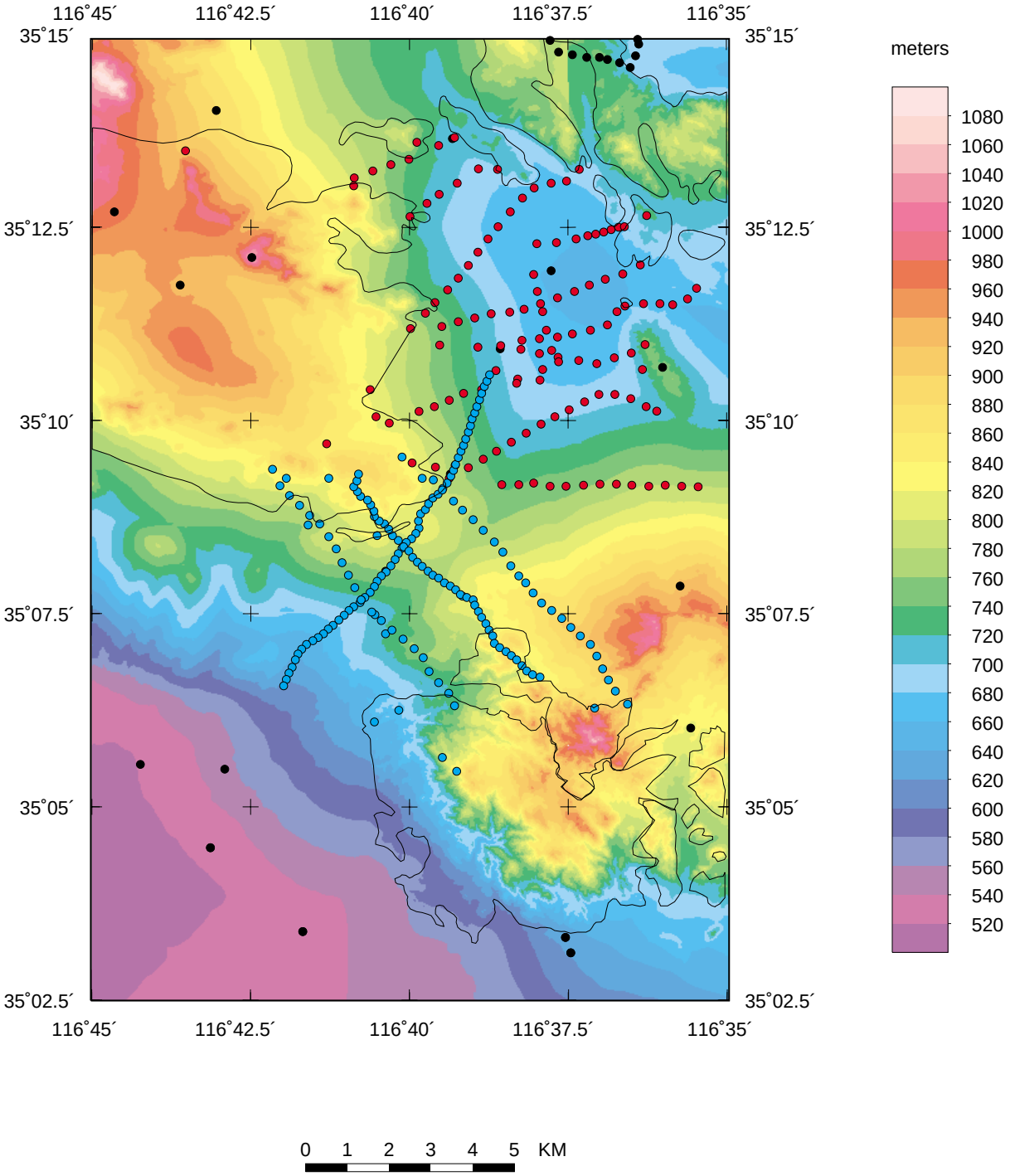

Figure 2. Location of gravity stations and outline of basement exposure shown on topographic map of study area. Black dots, pre–existing stations; red dots, stations collected in 1996; blue dots, stations colleced in 1999.

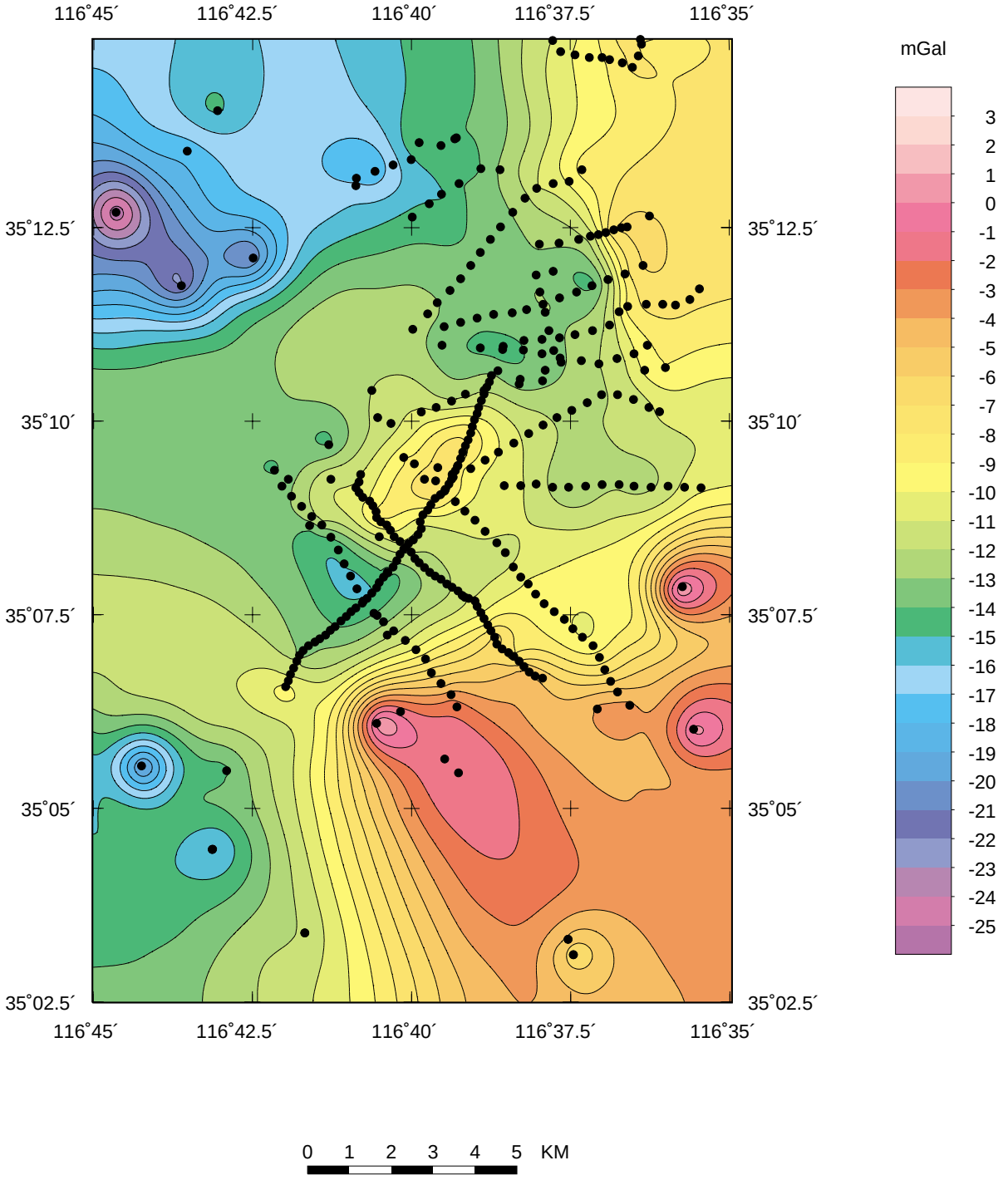

Figure 3. Isostatic gravity map of study area. Contour interval 1 mGal. Black dots, gravity stations.

Complete Bouguer anomalies were calculated by adding the terrain correction and the curvature correction to the simple Bouguer anomaly. The gravitational effects of terrain out to 166.7 km from each station were removed from observed gravity in three steps: field corrections for local terrain out to 68 m (Hayford and Bowie 1912); inner–zone corrections, for terrain between 68 m and 0.59 km (Hayford and Bowie 1912; Spielman and Ponce, 1984) using 30 m DEM's; and computer–based corrections (Plouff, 1966; Plouff, 1977; Godson and Plouff, 1988) for terrain between 0.59 km and 166.7 km.

These data were processed through an isostatic reduction program (Jachens and Roberts, 1981) in order to suppress the effects of deep density distributions that buoyantly support the topography. The isostatic reduction assumes an Airy–Heiskanen model with the following parameters from the station to 166.7 km: density of topography above sea level, 2.67 g/cm^3; crustal thickness at sea level, 25 km; density contrast across the base of the model crust, 0.4 g/cm^3. From 166.7 km to a point on the opposite side of the Earth, isostatic and terrain corrections were taken off maps by Karki (1961). These corrections were added to the output of the isostatic program of Jachens and Roberts (1981) to produce the isostatic correction. Isostatic anomalies are calculated by adding the isostatic correction to the complete Bouguer anomaly. The isostatic gravity map is shown in figure 3.

DEPTH–TO–BASEMENT

The depth to pre–Cenozoic basement beneath Langford Well Lake basin was calculated using gravity data, bedrock geology, and variable density of sediments. For this study area, basement consists mostly of Cretaceous and Jurassic plutons. Alvord Mountain, in the southern part of the study area, contains Tertiary volcanic basalts, which are considered basement for this exercise. Digitized polygons of basement outcrop were made using up–to–date geologic maps (David Miller, U.S. Geological Survey, written commun., 1998). These polygons are shown on figures 2, 4, and 5. The sediments are Quaternary and Tertiary in age.

PROCEDURE

Depth–to–basement was calculated using a method developed by Jachens and Moring (1990) and since updated to use constraining depth data such as wells that penetrate basement or seismic estimates of basin fill (Bruce Chuchel, U.S. Geological Survey, written commun., 1996). The gravity data are sorted into three files: measurements that lie on bedrock in the study area, measurements that lie on fill in the study area, and measurements that are outside the study area. Data outside the study area are used to avoid edge effects in this method. The procedure first calculates a grid based just on bedrock stations. In areas of basin fill, values derived from the grid are subtracted from actual measurements, and the difference is used to estimate the thickness of basin fill assuming a specified density–depth function. There are a couple of difficulties with this initial estimate: 1) Gravity observed at bedrock stations near the edge of the outcrops are lowered by the effect of the nearby low–density fill. 2) The lateral densities of the bedrock are not taken into account, which effects the basement gravity field. The lateral variations of the density of Cenozoic deposits are not taken into account in this inversion method.

To get around these problems, a smooth surface is fit through the basement gravity grid by interpolation, including locations where the basin thickness is known and using the density–depth function. The first estimate of basin thickness is made and used to correct the basement gravity at all gravity station locations. The basin thickness is forced to zero within the bedrock polygons. This gives a first approximation of the basement gravity. This process is repeated until the basement gravity shows no appreciable change.

DENSITY–DEPTH FUNCTION

The density–depth function allows for changes in density of Cenozoic deposits as a function of depth. Various density–depth functions were tried in order to match known or suspected physical properties of Cenozoic deposits in the Langford Well Lake basin. The density–depth functions list the density of each layer and the depth from the surface of the contact between each layer. The gravity data were reduced with a density of 2.67 g/cm^3. The depths used are in kilometers.

Unfortunately, there are very few absolute constraints in this basin (table 1). There are eight wells in the basin that were used, but only one, LW1 reaches basement and its depth is very shallow (32 m, 105 ft). There are also two seismic refraction lines with preliminary depth estimates. The location of the wells used and the seismic lines (line 1 and line 2) are shown on figure 4. The rest of the wells did not reach basement. Several density–depth functions were tried in order to determine a basin at least as deep as the wells that did not reach basement and consistent with seismic depths.

The Quaternary/Tertiary (Q/T) boundary is estimated to be at a depth of 0.13 km (Jill Densmore, U.S. Geological Survey, written commun., 1996). Friable Tertiary sandstone from a depth of about 240 m (800 ft) in LL1 well has a measured a dry bulk density of about 2.4 g/cm^3. The estimated depths to basement from seismic reflection are 171 m (560 ft) for line 1 and 287 m (940 ft) for line 2 (David Berger, U.S. Geological Survey, written commun., 1996).

Table 1 shows the results of the various density–depth functions. The table lists the well identification, depth drilled, the calculated depth based on the density–depth function, and the difference between the well depth and the calculated basin depth at the well location. Seismic information is also shown. Because most of the wells do not reach basement, the assumption is that the basin thickness at those locations is deeper than the bottom of the wells. Therefore, the density–depth function should produce a negative number in the difference column. The density–depth function should also produce basin depths at the locations of the seismic profiles that approximate those depths estimated from the seismic interpretation. The values in the difference column should be close to zero for the seismic locations.

The first density–depth function used in this study was originally developed for the Basin and Range (Jachens and Moring, 1990). This yielded a basin thickness much too shallow. Increasing sediment density increases basin thickness. The density–depth function developed from seismic lines 1 and 2, were

Table 1. Density–depth functions.
[Depths and differences in feet.]

Standard Density–Depth Function: 2.02, 2.12, 2.32, 2.42 g/cm³ 0.2, 0.6, 1.2 km					
Note	Well ID	Well Depth	Seismic Depth	Calculated Depth	Difference
	LX–1	586		259	327
	LL1	800		484	316
basement	LW1	105		26	79
	LP1	703		627	76
	LP2	702		457	245
	LP3	601		383	218
	TH–8	374		617	-243
	TH–10	301		440	-139
Line 1			560	357	203
Line 2 on lake			940	649	291

Based on Seismic Line 2					
Density–Depth Function: 1.33, 2.04, 2.32, 2.42 g/cm³ .02, 0.29, 1.2 km					
Note	Well ID	Well Depth	Seismic Depth	Calculated Depth	Difference
	LX–1	586		183	403
	LL1	800		410	390
basement	LW1	105		13	92
	LP1	703		547	156
	LP2	702		384	318
	LP3	601		308	293
	TH–8	374		538	-164
	TH–10	301		364	-63
Line 1			560	289	271
Line 2 on lake			940	564	376

Based on Seismic Line 1					
Density–Depth Function: 1.64, 1.80, 2.19, 2.35, 2.42 g/cm³ .02, .06, 0.17, 1.2 km					
Note	Well ID	Well Depth	Seismic Depth	Calculated Depth	Difference
	LX–1	586		177	409
	LL1	800		452	348
basement	LW1	105		16	89
	LP1	703		692	11
	LP2	702		416	286
	LP3	601		321	280
	TH–8	374		669	-295
	TH–10	301		390	-89
Line 1			560	292	268
Line 2 on lake			940	735	205

Table 1. Density–depth functions. —Continued

Based on Rock Sample and Q/T Boundary; no constraints					
Density–Depth Function: 2.17, 2.27, 2.37, 2.42 g/cm^3 0.13, 0.24, 0.6 km					
Note	Well ID	Well Depth	Seismic Depth	Calculated Depth	Difference
	LX–1	586		341	245
	LL1	800		689	111
basement	LW1	105		34	71
	LP1	703		1053	-350
	LP2	702		643	59
	LP3	601		525	76
	TH–8	374		1027	-653
	TH–10	301		617	-316
Line 1			560	479	81
Line 2 on lake			940	1152	-212

Based on Rock Sample and Q/T Boundary; using well					
Density–Depth Function: 2.17, 2.27, 2.37, 2.42 g/cm^3 0.13, 0.24, 0.6 km					
Note	Well ID	Well Depth	Seismic Depth	Calculated Depth	Difference
	LX–1	586		364	222
	LL1	800		702	98
basement force	LW1	105		103	2
	LP1	703		1056	-353
	LP2	702		653	49
	LP3	601		541	60
	TH–8	374		1040	-666
	TH–10	301		620	-319
Line 1			560	489	71
Line 2 on lake			940	1105	-165

Based on Rock Sample and Q/T Boundary; using well and forcing					
Density–Depth Function: 2.17, 2.27, 2.37, 2.42 g/cm^3 0.13, 0.24, 0.6 km					
Note	Well ID	Well Depth	Seismic Depth	Calculated Depth	Difference
force	LX–1	586		570	16
force	LL1	800		790	10
Basement force	LW1	105		104	1
	LP1	703		1112	-409
force	LP2	702		702	0
force	LP3	601		603	-2
	TH–8	374		1158	-784
	TH–10	301		692	-391
Line 1 force			560	558	2
Line 2 on lake force			940	964	-24

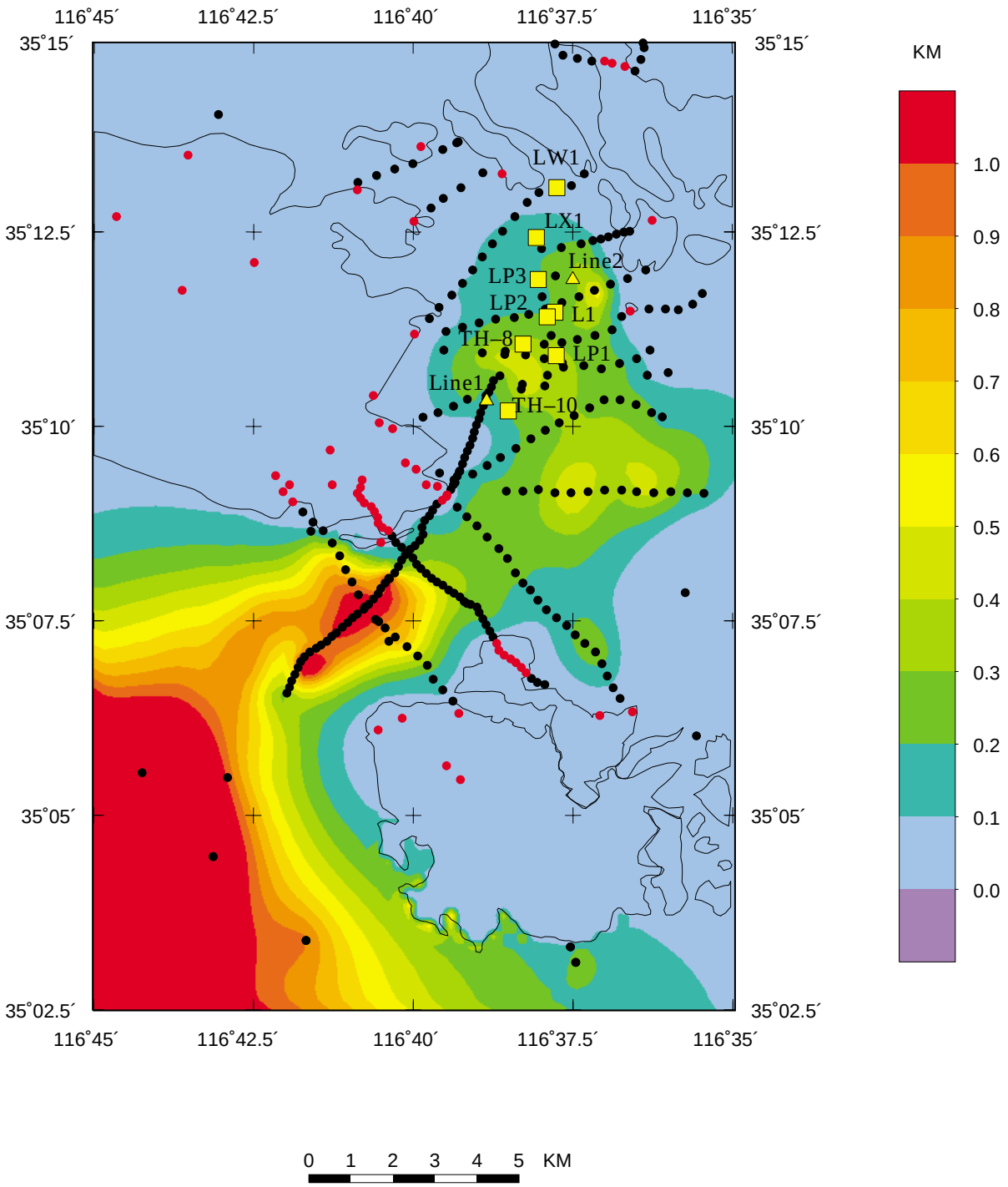

Figure 4. Depth–to–basement map of study area. Contour interval 0.1 km. Lines indicate basement geology. Red dots, basement gravity stations; black dots, basin gravity stations; yellow squares, well locations; yellow triangles, seismic lines.

based on velocity–depth cross sections (David Burger, U.S. Geological Survey, written commun., 1996). Although these velocities are unreasonably slow for basin fill sediments, and yielded depths much too shallow, the estimated depth of the basin, based on seismic refraction, seem realistic. Conversion of velocity to density was made by an equation of Gardener and others (1974).

Using the Q/T boundary estimate of 0.13 km provided the best fit. Quaternary sediments above this boundary were assigned a density of 2.17 g/cm^3 and Tertiary sediments below this boundary were assigned a density of 2.27 g/cm^3. The Tertiary sediments below 0.24 km were assigned a density of 2.37 g/cm^3, which reflects the measured density of a core sample at the bottom of the LL1 well. These results placed the basement near or below the depths of the wells and the seismic depths. By forcing the LW1 well to basement, all of the differences became smaller except seismic line 2, which also is an improvement. The final step was to force all of the wells whose differences were not negative to the drill depths. Because these wells did not reach basement they could have been forced deeper, but a more conservative approach was not to force the depths deeper than is known. The seismic depths were forced to fit.

CONCLUSIONS

The resulting basement thickness grid is shown in figure 4. A structure map is shown in figure 5, calculated by subtracting the depth–to–basement from topography. The resultant map is a structural contour map of the basement surface. Figure 5 essentially is a topographic map of the study area with sediments removed.

Langford Well Lake basin, based on current data, contains three sub–basins. A small sub–basin lies under the lakebed, as expected. A much broader but shallower sub–basin lies southwest of the lakebed. Although not as deep, it is of much larger area. An arc–shaped basin about the same size as the middle basin lies 4.5 km south of the lakebed. The entire Langford Well Lake basin is closed at about the 500–m level and spills to the Coyote Lake basin to the southwest.

Wells LP1, LP2, LL1, LP3, and LX–1 are aligned in a row on what appears to be a ridge between the north basin and the middle basin. Although well TH–8 is not very deep, the calculated depth of the basin is over 335 m (1,100 f) deep at that well site, which is located just north of the middle basin. The southern basin has very poor control. It appears to be at least as deep as the middle basin, but additional gravity stations are needed to better delineate its size and depth.

Locations of maxima in maximum horizontal gravity gradients are shown in figure 6. The steepest horizontal gradients of gravity anomalies caused by a tabular body tend to lie directly over the edge of the bodies if the edges of the bodies are vertical and far enough away from other sources. A procedure of Cordell (1979) uses the lateral variation of gravity anomalies to extract gradients of density directly from gravity measurements. Juxtaposed rocks of contrasting densities cause these gradients. These boundaries can be caused by geologic contacts or faulting. Mapped faults are also shown on this map. There is good correlation between some of the mapped faults and some of the maxima of gradients. Dashed lines emphasize linear trends inferred from these gradient maxima which could be extensions of faults not visible at the surface. The gradient maxima shown in figure 6 may be useful as evidence of additional faulting in this study area.

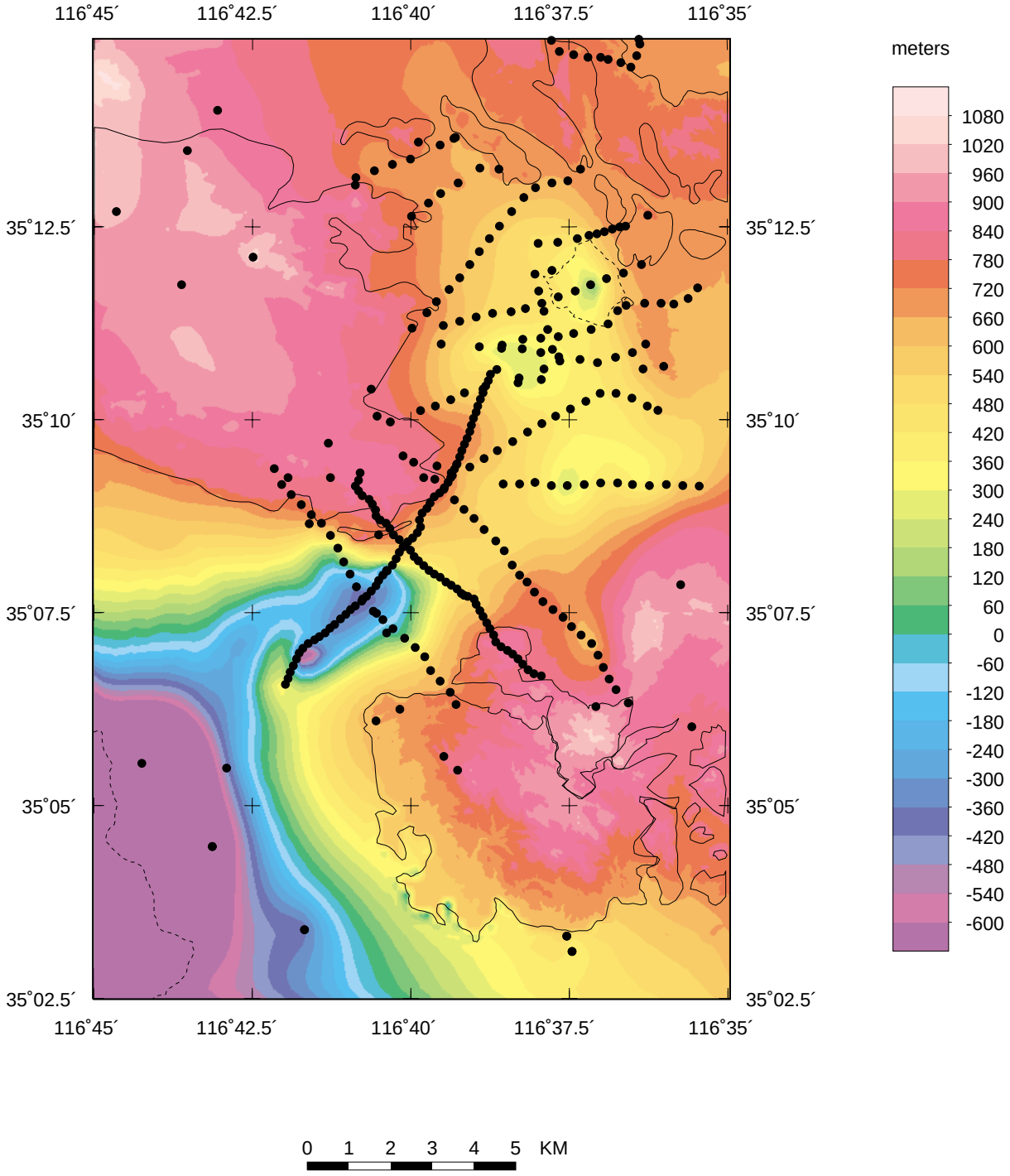

Figure 5. Structural contour map of study area. Contour interval 60 m relative to sea level. Black dots, gravity stations; dashed lines, lake beds; solid lines, basement geology.

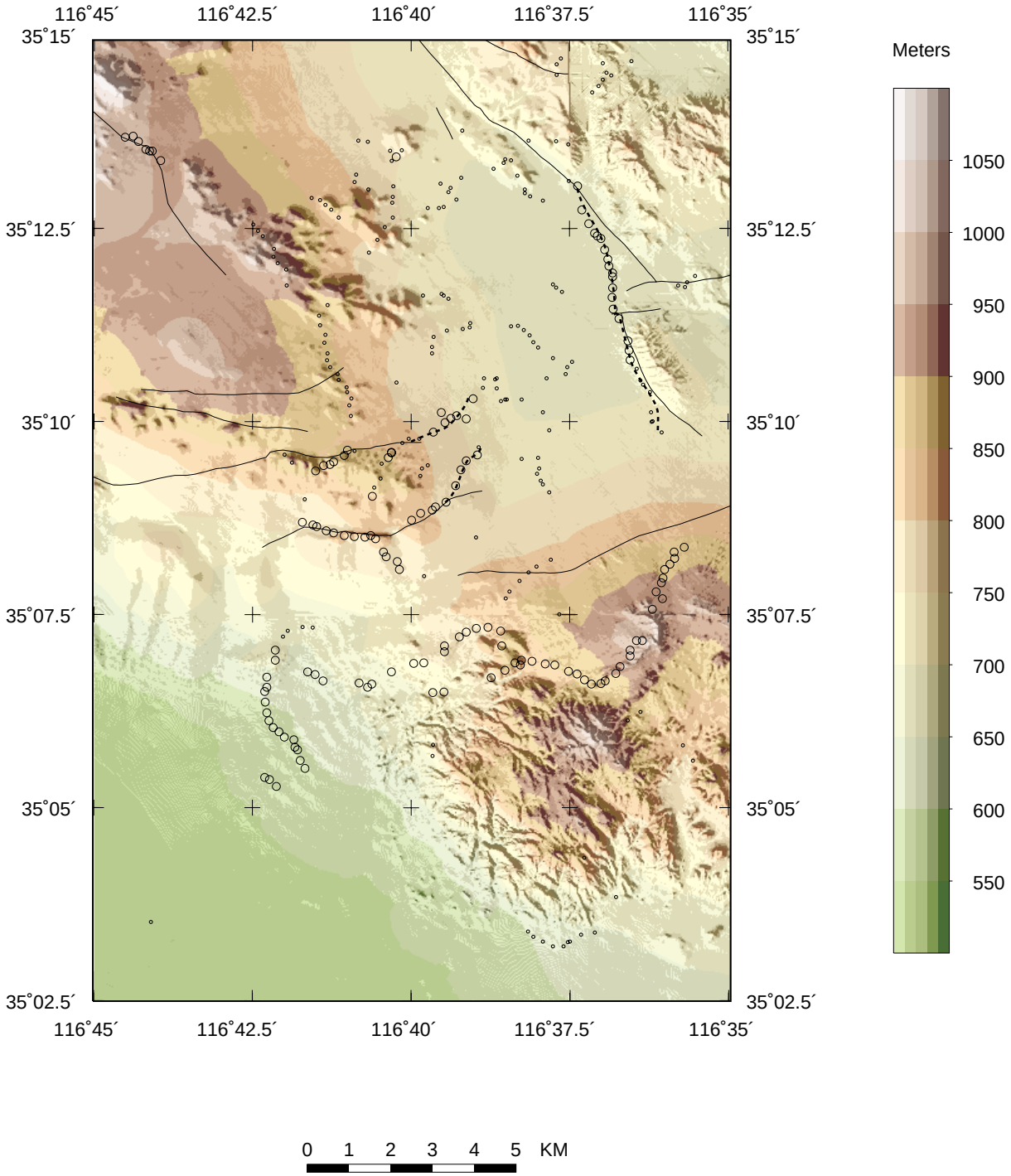

Figure 6. Location of maxima in maximum horizontal gravity gradient shown on topographic base. Black lines, mapped faults; small open circles, gradient maxima between 1 and 3 mGal/km; large open circles, gradient maxima between 3 and 8 mGal/km; dashed lines, possible locations of faults inferred from gradients.

REFERENCES CITED

Barnes, D. F., Oliver, H.W., and Robbins, S.L., 1969, Standardization of gravimeter calibrations in the Geological Survey: Eos (American Geophysical Union Transactions), v. 50, no. 10, p. 626–527.

Cordell, L., 1979, Gravimetric expression of graben faulting in Santa Fe country and the Española Basin, New Mexico, *in* Ingersoll, R.V. (ed.) Guidebook to Santa Fe Country, 30th Field Conference: New Mexico Geological Society, 59–64.

Gardner, G.H.F., Gardner L.W., and Gregory A.R., 1974, Formation velocity and density; the diagnostic basics for stratigraphic traps: Geophysics, 39, 770–780.

Godson, R.H., and Plouff, Donald, 1988, BOUGUER version 1.0, a microcomputer gravity–terrain–correction program: U.S. Geological Survey Open–File Report 88–644–A, Documentation, 22 p.; 88–644–B, Tables, 61 p., 88–644–C, 5 1/4–inch diskette.

Hayford, J.F., and Bowie, William, 1912, The effect of topography and isostatic compensation upon the intensity of gravity: U.S. Coast and Geodetic Survey Special Publication no. 10, 132 p.

International Association of Geodesy, 1971, Geodetic reference system 1967: International Association of Geodesy Special Publication No. 3, 116p.

Jachens, R.C., and Roberts, C.W., 1981, Documentation of a FORTRAN program, 'isocomp', for computing isostatic residual gravity: U.S. Geological Survey Open–File Report 81–574, 26 p.

Jachens, R.C., and Moring, B.C., 1990, Maps of thickness of Cenozoic deposits and the isostatic residual gravity over basement for Nevada: U.S. Geological Survey Open–File Report 90–404.

Karki, Pentti, Kivioja, Lassi, and Heiskanen, W.A., 1961, Topographic isostatic reduction maps for the world for the Hayford Zones 18–1, Airy–Heiskanen System, T=30 km: Publication of the Isostatic Institute of the International Association of Geodesy, no. 35, 5p., 20 pl.

Morelli, C., ed, 1974, the International gravity standardization net 1971: International Association of Geodesy Special Publication no. 4, 194 p.

Plouff, Donald, 1966, Digital terrain corrections based on geographic coordinates [abs.]: Geophysics, v. 31, no. 6, p. 1208.

Plouff, Donald, 1977, Preliminary documentation for a FORTRAN program to compute gravity terrain corrections based on topography digitized on a geographic grid: U.S. Geological Survey Open–File Report 77–535, 45 p.

Spielman, J.B., and Ponce, D.A., 1984, HANDTC, a FORTRAN program to calculate inner–zone terrain corrections: U.S. Geological Survey Open–file Report 84–777, 20 p.

Swick, C.H., 1942, Pendulum gravity measurements and isostatic reductions: U.S. Coast and Geodetic Survey Special Publication no. 232, 82 p.